JOURNAL OF THERMOPHYSICS AND HEAT TRANSFER
Vol. 10, No. 3, July–September 1996

Nonequilibrium Vibrational Kinetics in the Boundary Layer of Re-Entering Bodies

I. Armenise,* M. Capitelli,† G. Colonna,‡ and C. Gorse†
University of Bari, Bari 70126, Italy

Nonequilibrium vibrational distributions of N_2 in the boundary layer surrounding a blunt body in hypersonic flow have been calculated by coupling the nonequilibrium vibrational kinetics, the dissociation and recombination processes, and the boundary-layer equations. The role of different energy exchange processes [vibration–vibration (V–V), vibration–translation (V–T), and recombination–dissociation] in affecting vibrational kinetics has been studied by considering each process. Then the complete kinetics are taken into account, obtaining a global view of the interplay of the different microscopic processes. The model used for the recombination/dissociation processes is such to selectively pump levels $v = 25$ and 45 of the N_2 vibrational manifold. This vibrational energy is then redistributed by V–V and V–T processes. As a result, strongly nonequilibrium vibrational distributions are obtained, despite the thermalizing action of the V–T processes by nitrogen atoms.

Nomenclature

c_p = specific heat at constant pressure including only rotational and translational degrees of freedom
c_v = $\rho_v(\eta)/\rho(\eta)$
E_i = total energy of the ith state
$E_{q,w\to v}$ = energy of the process $w \to v$
$f(\eta)$ = stream function
g_i = statistical weight of the ith state, related to level multiplicity
K_{eq} = equilibrium constant
k = Boltzmann constant
Le = Lewis number
l = $\rho\mu/(\rho\mu)_e$
Pr = Prandtl number
p = pressure inside the boundary layer
p_e = pressure at the edge of the boundary layer
p_∞ = pressure outside the shock layer
R = nose radius
$R_{q,d,w\to v}$ = volume rate coefficient
$R'_{q,d,w\to v}$ = mass rate coefficient
Sc = Schmidt number
T = local translational temperature
T_e = temperature at the edge of the boundary layer
T_w = wall temperature
u_e = longitudinal speed at the edge of the boundary layer
x, ξ = body-parallel coordinates
y, η = body-normal coordinates
β = du_e/dx
η_{max} = value of η at the edge of the boundary layer
θ = $T(\eta)/T_e$
μ = local viscosity coefficient
μ_e = viscosity coefficient at the edge of the boundary layer
ρ_e = mass density at the edge of the boundary layer
$\rho_v(\eta)$ = local mass density of molecules in the vth vibrational state
$\rho(\eta)$ = local total mass density

Received Jan. 5, 1995; revision received June 21, 1995; accepted for publication Dec. 7, 1995.

*Researcher, Centro di Studio per la Chimica dei Plasmi del CNR, Department of Chemistry.
†Professor, Centro di Studio per la Chimica dei Plasmi del CNR, Department of Chemistry.
‡Researcher, Centro di Studio per la Chimica dei Plasmi del CNR, Department of Farmaceuticol-Chemistry.

I. Introduction

NONEQUILIBRIUM vibrational distributions of N_2 have been widely investigated in recent years because of their importance in affecting the properties of N_2 when the vibrational temperature is much higher than the translational one. These conditions occur in cold plasmas where electrons pump vibrational energy into the low-lying vibrational levels of N_2 while vibration–vibration (V–V) energy exchange processes redistribute the introduced quanta over the whole vibrational ladder of N_2, ending under specific conditions in dissociation.[1] The corresponding vibrational distribution is characterized by the so-called Treanor distribution over the first few vibrational levels, by a plateau over intermediate levels and by a tail, which is the result of the interplay of V–V and vibration–translation (V–T) energy exchange processes.

Another possibility to obtain similar nonequilibrium vibrational distributions is to consider postdischarge conditions[1]: we can pump vibrational energy by electrons in the electrical discharge and then allow the redistribution of vibrational quanta in the postdischarge, again obtaining highly nonequilibrium vibrational distributions.

A third way to obtain nonequilibrium vibrational distributions is to heat high-pressure N_2 to high temperature and then expand it through a nozzle, decreasing the translational temperature: in this case the system can achieve strongly nonequilibrium vibrational distributions as a result of the interplay of V–V and V–T energy transfer processes.[1]

Similar conditions can be achieved during the re-entry in the atmosphere of space vehicles at hypersonic speed. During the interaction with the vehicle, the surrounding air not only can achieve very high translational temperatures, but also dissociates and ionizes. The vehicle is surrounded by a boundary layer characterized by a high-edge temperature T_e, which degradates toward the temperature of the vehicle surface T_w. Atoms and vibrationally excited molecules diffuse through this gradient, undergoing energy redistribution processes. If the characteristic time of these processes has the same order of magnitude as the characteristic residence time in the boundary layer, the kinetics cannot be disregarded. In this case a complicated model that couples kinetics and fluid dynamics must

be used to understand the different phenomena occurring in the flow.

Usually two approaches are followed: the first one emphasizes the fluid dynamic aspects by solving the complete Navier–Stokes equations and by assigning different temperatures (translational, rotational, vibrational, and electronic) to each degree of freedom. As an example, the whole vibrational manifold of the diatomic molecule is represented by an equation for the vibrational temperature, implying that a Boltzmann distribution holds for the vibrational levels.

The second approach emphasizes the kinetics in the sense that the vibrational manifold of the molecule is treated as composed by a given number of energy levels, each of which is considered as a different chemical species. The fluid dynamics is simplified by solving the boundary-layer (BL) equations: under this assumption the body-parallel and body-normal flow are separated, giving the possibility to consider very complicated kinetics. This approach allows us to determine the deviation of the vibrational distributions from the Boltzmann ones.

In this article we will follow the latter approach developed and applied for the first time some years ago by Doroshenko et al.[2] These authors were mainly concerned with the effect of nonequilibrium vibrational distributions on the heat transfer to the vehicle surface, an important engineering problem (see also Ref. 3). On the contrary, the aim of our work is to show the nonequilibrium character of the vibrational distributions of N_2 along the coordinate perpendicular to the surface of the vehicle and its dependence on the sets of rate coefficients describing the V–V and V–T processes.

To completely understand the problem we will consider only the vibrational distribution of pure nitrogen under the presence of the dissociation–recombination process as well as under the action of V–V and V–T energy exchange processes, i.e., we completely neglect the presence of atomic and molecular oxygen in the boundary layer. Moreover, contrary to our previous works, the recombination–dissociation process is considered as a macroscopic process that selectively populates (and depopulates) given vibrational levels.

We also do not consider the possibility of conversion of vibrational energy into electronic energy, as well as the presence of free electrons.

II. Numerical Model

To study the boundary-layer vibrational kinetics of the hypersonic re-entry vehicles, it is necessary to solve the relevant BL equations. To put in evidence the role of the vibrational kinetics, we choose the simplest flow (axisymmetric or unlimited in one direction), and we use the stagnation point approximation.[2–4] In this case, the flow is two dimensional, and it is useful to use general coordinates by performing the Lees–Dorodnitsyn transformation[2] (see also Chaps. 5 and 6 of Ref. 4):

$$\xi = \int_0^x \rho_e(x')u_e(x')\,dx' \qquad \eta = \frac{u_e(x)}{\sqrt{2\xi}} \int_0^y \rho(y')\,dy' \tag{1}$$

In these general coordinates BL equations are separable in different contributions. The first is for $f(\eta)$, which for the flat plate case can be written as (Ref. 2) (see also Chap. 6 of Ref. 4):

$$\frac{\partial}{\partial \eta}\left[\frac{\rho\mu}{\rho_e\mu_e}\frac{\partial^2 f(\eta)}{\partial \eta^2}\right] + f(\eta)\frac{\partial^2 f(\eta)}{\partial \eta^2} = 0 \tag{2}$$

$$\frac{u(\eta)}{u_e} = \frac{\partial f(\eta)}{\partial \eta} \tag{3}$$

The stream function gives the contribution of the body-parallel flow to the body-normal flow equations. Numerical solution[5] of Eq. (2) for $\rho\mu/(\rho\mu)_e = 1$ can be expressed as

$$f(\eta) = \max(0, -0.3316 + 0.4908\eta + 0.0427\eta^2) \tag{4}$$

The range of η has values between 0 (at the surface) and $\eta_{\max}$ (at the edge of the boundary layer).

The equations for the body-normal flow are (Ref. 2) (see also Chap. 17 of Ref. 4)

$$l\frac{\partial^2 \theta}{\partial \eta^2} + Prf(\eta)\frac{\partial \theta}{\partial \eta} = -LeS_\theta \tag{5}$$

for the reduced translational temperature and

$$l\frac{\partial^2 c_v}{\partial \eta^2} + Scf(\eta)\frac{\partial c_v}{\partial \eta} = -S_v \tag{6}$$

for mass concentration. In our model these numbers are considered constant with values $Pr = 0.71$, $Sc = 0.49$, $Le = 1.45$, and $l = 1$.

The functions θ and c_v are, respectively, the normalized temperature and mass concentration, i.e.,

$$\theta(\eta) = [T(\eta)/T_e] \qquad c_v(\eta) = \rho_v(\eta)/\rho(\eta) \tag{7}$$

The terms on the right in Eqs. (5) and (6) are sources from molecular collision processes (e.g., V–V and V–T energy exchange processes, dissociation or recombination), and have the form

$$S_v = a\sum_{q,w,d}^{N}(R'_{q,d,w\to v}c_w c_d - R'_{q,d,v\to w}c_v c'_d) \tag{8}$$

$$S_\theta = a\sum_{q,d,w}^{N}\left(\frac{E_{q,w\to v}}{c_p T_e}\right)(R'_{q,d,w\to v}c_w c_d - R'_{q,d,v\to w}c_v c'_d) \tag{9}$$

with

$$a = \frac{pSc}{kT(1+J)\beta\sum_w c_w} \tag{10}$$

$$R'_{q,d,w\to v} = R_{q,d,w\to v}\frac{\rho kT}{pm_w} \tag{11}$$

Together with Eqs. (5) and (6), it is necessary to consider the boundary conditions that take into account the physical quantities outside the boundary layer and the heat exchange and catalytic processes on the space vehicle surface. In our particular case we suppose that outside the boundary layer the temperature is constant ($T = T_e$). We assume that a Boltzmann vibrational distribution as well as an equilibrium composition of atoms and molecules hold at $T = T_e$. The surface ($\eta = 0$) is assumed to be at a constant temperature $T(\eta = 0) = T_w$ and to be noncatalytic to both atom recombination and vibrational energy accommodation, i.e.,

$$T(0) = T_w \quad T(\eta_{\max}) = T_e \quad \frac{dc_v(0)}{d\eta} = 0 \quad c_v(\eta_{\max}) = c_0 e^{-E_v/kT_e} \tag{12}$$

Therefore, the model is described by a system of nonlinear, coupled, parabolic differential equations (46 for the vibrational states, 1 for atoms, and 1 for gas temperature) with two boundary conditions. The numerical code used reaches the solution through the following steps:

1) The calculation of the temperature profile and the vibrational distribution in the collisionless regime (the source terms are all null).

2) The calculation of the source terms with the old temperature profile and vibrational distribution.

3) The calculation of new temperature profile and the spatial profile for each vibrationally excited molecule.

4) The normalization of the local vibrational distribution.

5) The control of the variations in the vibrational distribution; if they are greater than a certain value, go back to point 2, otherwise stop the calculation.

In this work we calculate the distribution in pure nitrogen considering the following collisional processes:

V–V energy exchange processes:

$$N_2(v) + N_2(w) \rightarrow N_2(v-1) + N_2(w+1) \tag{13}$$

V–T energy exchange by collisions with molecules:

$$N_2(v) + N_2 \rightleftarrows N_2(v-1) + N_2 \tag{14}$$

V–T energy exchange by collisions with atoms:

$$N_2(v) + N \rightleftarrows N_2(v-\Delta v) + N \tag{15}$$

Dissociation:

$$N_2(v) + \begin{matrix} N \\ N_2 \end{matrix} \rightarrow 2N + \begin{matrix} N \\ N_2 \end{matrix} \tag{16}$$

Recombination:

$$2N + \begin{matrix} N \\ N_2 \end{matrix} \rightarrow N_2(v) + \begin{matrix} N \\ N_2 \end{matrix} \tag{17}$$

The rate coefficients R of the relevant processes are inserted in the codes as analytical expressions of the starting and arrival vibrational level and translational temperature (supposing that the rotational degree of freedom is in equilibrium with the translational one), and for reversal processes have been applied detailed balance principle, i.e.,

$$R_{2\rightarrow 1} = (g_1/g_2)R_{1\rightarrow 2} \exp[(E_2 - E_1)/kT] \tag{18}$$

The expressions for the rate coefficients in cm^3s^{-1} are

$$R_{v\rightarrow v-1}^{w-1\rightarrow w} = 2.5 \times 10^{-14} vw(T/300)^{3/2} e^{-\delta_w|v-w|} \times (1.5 - 0.5e^{-\delta_w|v-w|}) \text{ for } w \leq v \text{ with } \delta_w = 6.8/\sqrt{T} \tag{19}$$

for V–V collisions,[2]

$$R_{v\rightarrow v-1} = vR_{1,0}e^{\delta_{vT}(v-1)}$$
$$\delta_{vT} = 0.26679 - 6.99237 \times 10^{-5}T + 6.99237 \times 10^{-5}T^2 \tag{20}$$
$$R_{1,0} = \exp[-3.24093 - (14{,}069{,}597/T^{0.2})]$$

for the V–T energy transfer by molecules, calculated with the aid of Billing et al.[6] rates.

The V–T energy transfer rates involving nitrogen atoms have been calculated according to the following equation:

$$R_{v\rightarrow w} = e^{a_0+a_1v} \quad \text{with} \quad v > w$$
$$\text{where } a_i = \sum_{k=0}^{2} \left(b_{i,k} + \frac{c_{i,k}}{T}\right)(v-w)^k \tag{21}$$

Table 1 Coefficients $b_{i,k}$ in Eq. (21)

i/k	0	1	2
0	−25.708	−0.1554	0.0054
1	0.0536	0.0013	-1.197×10^{-4}

Table 2 Coefficients $c_{i,k}$ in Eq. (21)

i/k	0	1	2
0	−5633.1543	111.3426	−2.189
1	122.4835	−4.2365	0.0807

the parameters of which obtained by using the semiclassical rates calculated by Laganà et al.[7,8]

The relevant $b_{i,k}$ and $c_{i,k}$ coefficients have been reported in Tables 1 and 2.

The following expression has been used for calculating the total dissociation rate ($cm^3s^{-1}mol^{-1}$)

$$R_{D,\text{tot}} = A \exp[-(113{,}200/T)]\{1 - \exp[-(3354/T)]\} \tag{22}$$

where A is a constant equal to 3.2×10^{16} for collisions with molecules and 7.2×10^{16} for collisions with atoms (Doroshenko et al.[2]).

The total recombination rate is then calculated through detailed balance

$$R_r = R_d/K_{\text{eq}} \tag{23}$$

where the equilibrium constant (mol/cm^3) is given by the following expression:

$$\ell n(K_{\text{eq}}) = -(112{,}361/T) + 1.6759 \times 10^{-4}T + 1.27790 \tag{24}$$

obtained by using the values tabulated by Park.[9]

The dependence of recombination on the vibrational level is obtained following Doroshenko et al.[2] According to these authors we assume that the recombination process selectively pumps levels $v = 25$ and $v = 45$ with statistical weights, respectively, of $\frac{3}{4}$ and $\frac{1}{4}$, i.e.,

$$\begin{aligned} R_{r,v} &= \tfrac{3}{4}R_r \qquad v = 25 \\ R_{r,v} &= \tfrac{1}{4}R_r \qquad v = 45 \\ R_{r,v} &= 0 \quad \text{all other} \quad v \end{aligned} \tag{25}$$

similarly for the dissociation rate.

This mechanism reflects the fact that during recombination the last vibrational level ($v = 45$) of the ground electronic state of the molecule ($X^1\Sigma_g^+$), as well as the excited electronic state ($A^3\Sigma_u^+$), are populated. The last, being resonant with the vibrational level $v = 25$ of $X^1\Sigma_g^+$, transfers its energy to this state. The weights $\frac{3}{4}$ and $\frac{1}{4}$ take into account the different multiplicities of the two electronic states.

We use an anharmonic oscillator with 45 bound levels, in agreement with previous results.[1] Insertion of more levels (up to 65) does not appreciably change the results, as recently shown in Ref. 3.

III. Results

Before considering the numerical results, we want to discuss the parameters that appear in the theory.

We start with β, which represents the gradient of velocity at the stagnation point of the vehicle and which can be considered in our model as representative of the residence time of the molecules in the boundary layer. The other two parameters are represented by T_e and T_w, i.e., by the values of temperatures at the edge of the boundary layer and at the surface of the vehicle as well as p, the pressure in the boundary layer.

In the present work, β, T_e, T_w, and p are considered as purely independent parameters: their variation covers a wide interval, in some cases we use values that are not realistic.

As an example, in Table 3 we have reported β values as a function of realistic Mach numbers for different R at an altitude of about 80 km, calculated according to the following equation (see Chap. 17 of Ref. 4):

$$\beta = (1/R) \times \sqrt{[2(p_e - p_\infty)/\rho_e]} \tag{26}$$

Moreover, to understand the results we will show the vibrational distributions calculated using the different processes separately, as well as including all processes together.

Let us start our discussion with temperature profiles.

$T(\eta)$ depends on the different assumptions we are making so that the actual profile is strictly linked to the self-consistent solution of Eqs. (5) and (6). Typical temperature profiles are reported in Figs. 1a and 1b for some of the conditions studied in this article (approximately for a Mach number of about 25). In particular, Fig. 1a reports the temperature profiles when the vibrational kinetics include only V–V and V–T terms, and Fig. 1b plots the corresponding profiles for the complete kinetic model (i.e., including V–V and V–T terms as well as the dissociation recombination kinetics). The differences between the various profiles are evident and are partially responsible for the different behavior of the nonequilibrium vibrational distributions in the boundary layer.

Table 3 Values of β (s^{-1}) as a function of Mach number for different R

Mach number	β			
	R = 0.1 m	R = 0.3 m	R = 0.5 m	R = 1 m
10	15,235	5,078	3,047	1,523
15	22,612	7,537	4,522	2,261
20	30,034	10,011	6,007	3,003
25	37,476	12,492	7,495	3,748
28	41,946	13,982	8,389	4,195

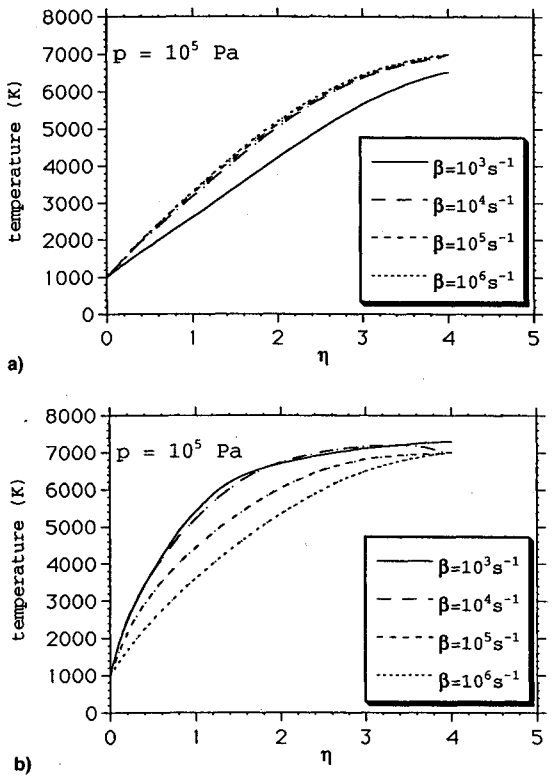

Fig. 1 Temperature profiles vs η for different p and β values in two different kinetic models: a) including only V–V and V–T processes and b) complete kinetic model.

The understanding of the present results is facilitated if one considers the typical vibrational distributions one expects as a result of the interplay of the different elementary processes.[1]

At high temperature, in the absence of a recombination–dissociation process, we can expect that the V–T processes

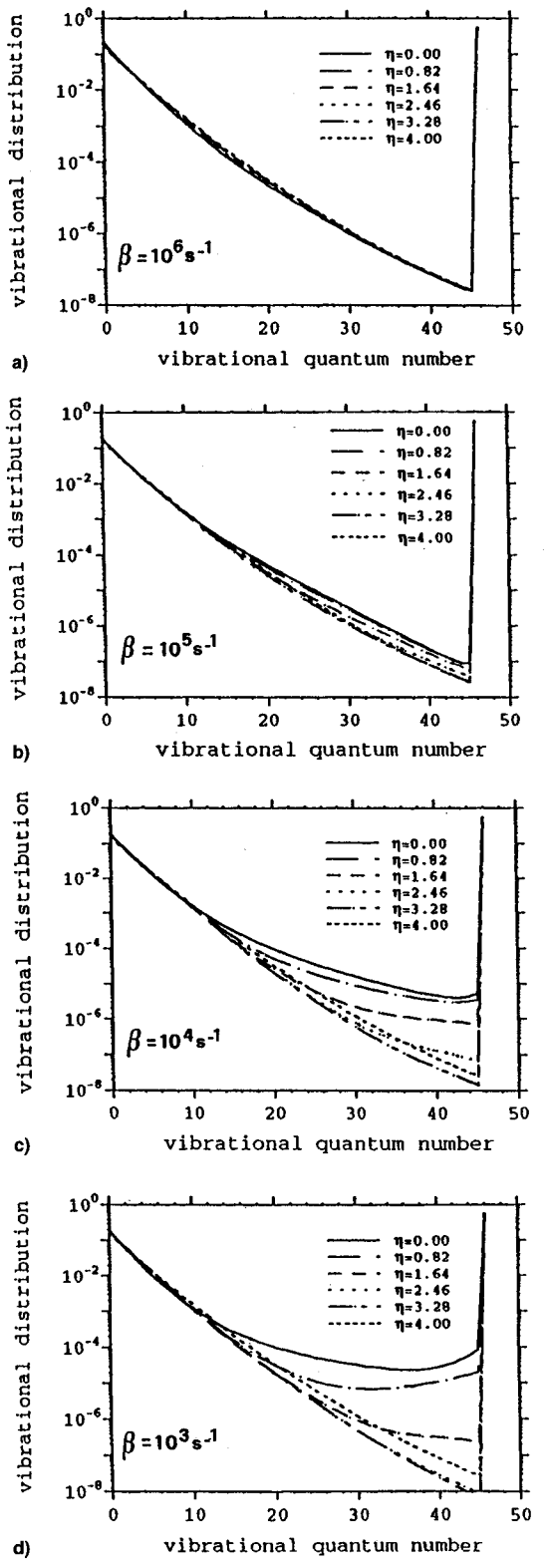

Fig. 2 Vibrational distributions vs vibrational quantum number at different η positions at fixed pressure (p = 10^5 N/m^2) and different β values calculated inserting only V–V energy exchange processes (T_e = 7000 K and T_w = 1000 K).

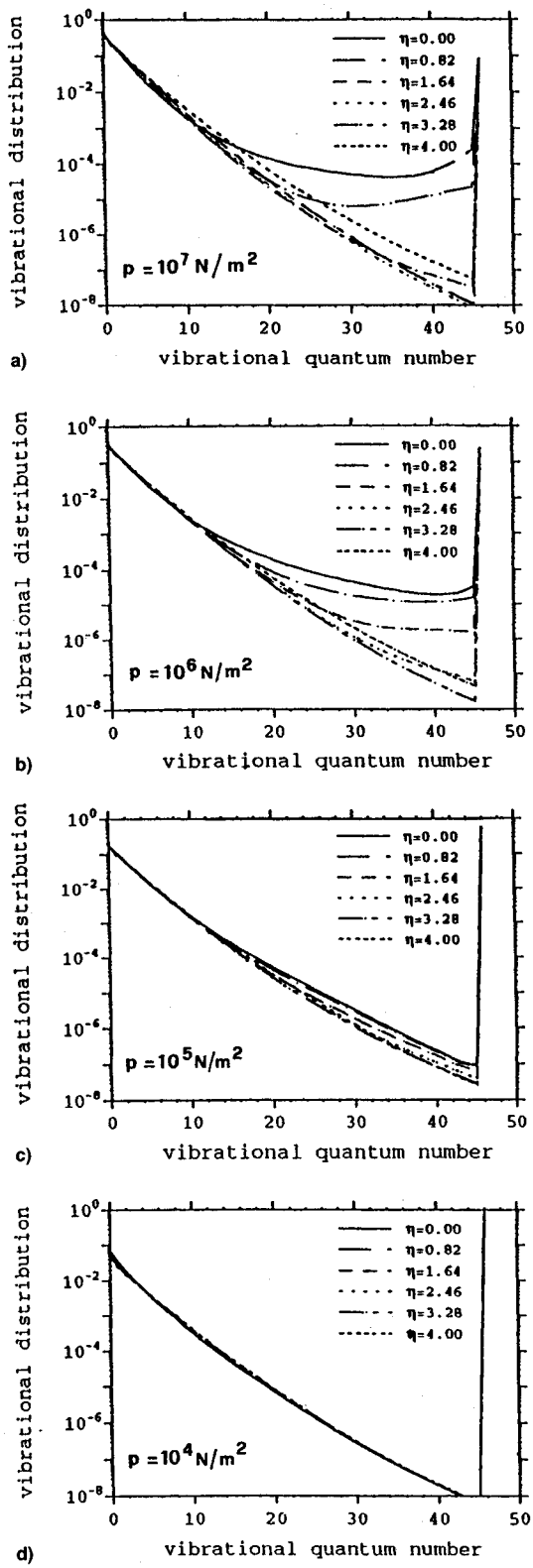

Fig. 3 Vibrational distributions vs vibrational quantum number at different η positions at fixed β ($\beta = 10^5$ s^{-1}) and different pressures calculated inserting only V–V energy exchange processes ($T_e = 7000$ K and $T_w = 1000$ K).

dominate the V–V ones, causing a Boltzmann distribution at the local gas temperature. A Boltzmann distribution appears as a straight line when plotting the logarithm of the concentration vs the vibrational quantum number.

On the other hand, near the low-temperature surface, the vibrational temperature of the low-lying levels T_1 may be much higher than the translational temperature. These conditions typically cause a Treanor distribution, which is characterized by a minimum in the vibrational distribution.

When V–T energy exchange processes occur, these distributions can have a long plateau at the intermediate levels where quasiresonant V–V energy exchange processes dominate and a tail for levels near the continuum.

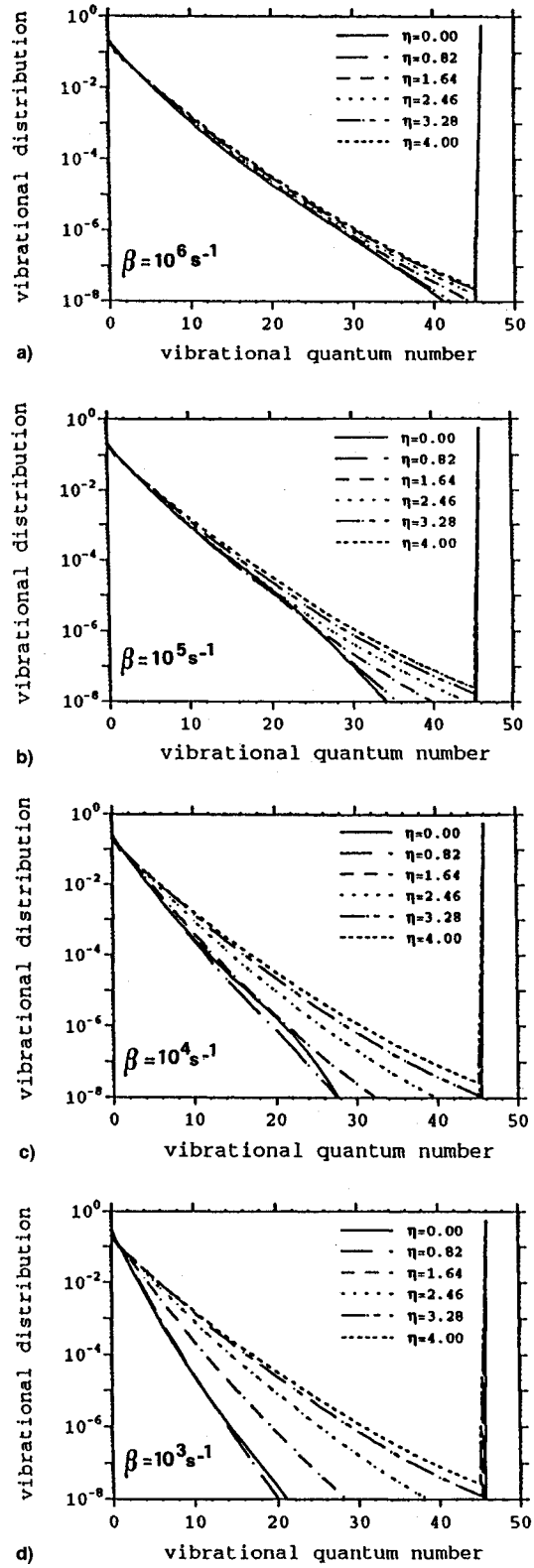

Fig. 4 Vibrational distributions vs vibrational quantum number at different η positions at fixed pressure ($p = 10^5$ N/m^2) and different β values calculated inserting only V–V and V–T (by molecules) energy exchange processes ($T_e = 7000$ K and $T_w = 1000$ K).

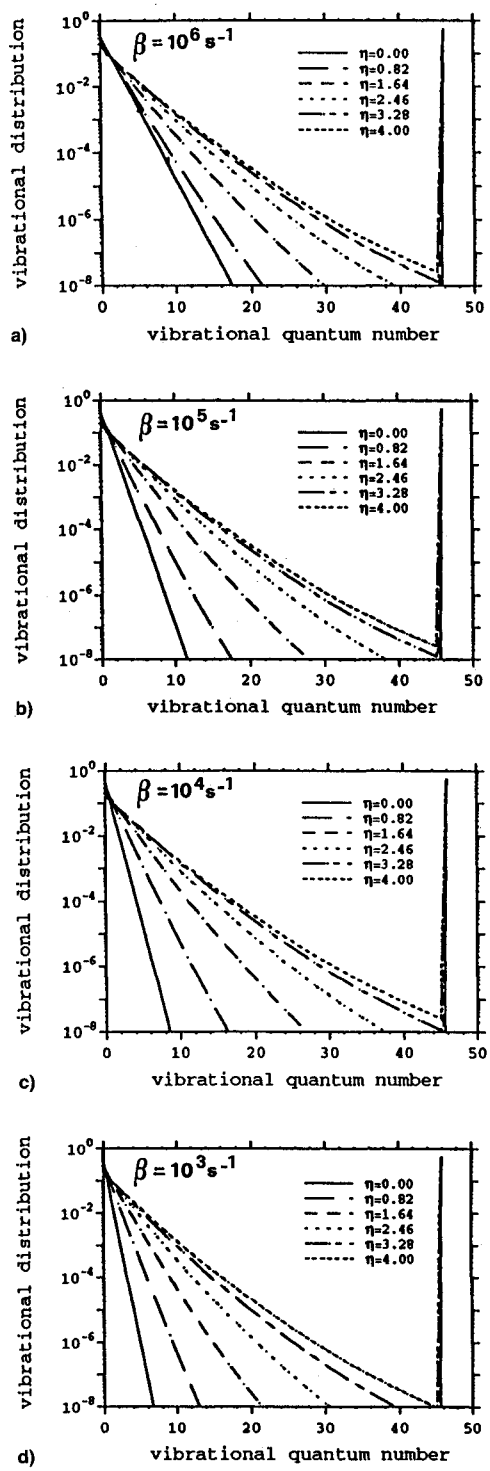

Fig. 5 Vibrational distributions vs vibrational quantum number at different η positions at fixed pressure ($p = 10^5$ N/m^2) and different β values calculated inserting only V–V and V–T (by both atoms and molecules) energy exchange processes ($T_t = 7000$ K and $T_v = 1000$ K).

Finally, in the presence of the recombination process, which selectively populates given vibrational levels, a new plateau can be formed as a result of this pumping mechanism followed by V–T redistribution. This mechanism can also increase the dissociation as pointed out in Ref. 1.

The form of a given distribution strongly depends on the temperature profile as well as on the selection of the elementary processes used in the vibrational kinetics.

Keeping in mind the previous qualitative observations, we can discuss the results. We first examine the nonequilibrium vibrational distributions at different β values along the η coordinate, calculated by using only the V–V processes (remember that $\eta = 0$ and $\eta = \eta_{max}$ refers, respectively, to the vehicle surface and to the boundary-layer edge). $\eta_{max} = 4$ is used; calculations with $\eta_{max} > 4$ do not yield appreciable differences.

Figures 2a–2d report the vibrational distributions at different η for $p = 10^5$ Nm^{-2} and β ranging from 10^6 to 10^3 s^{-1}. It can be observed that typical vibrational distributions in presence of V–V processes clearly appear for values $\beta < 10^5$ s^{-1}. This means that for $\beta > 10^5$ s^{-1}, the vibrational kinetics are

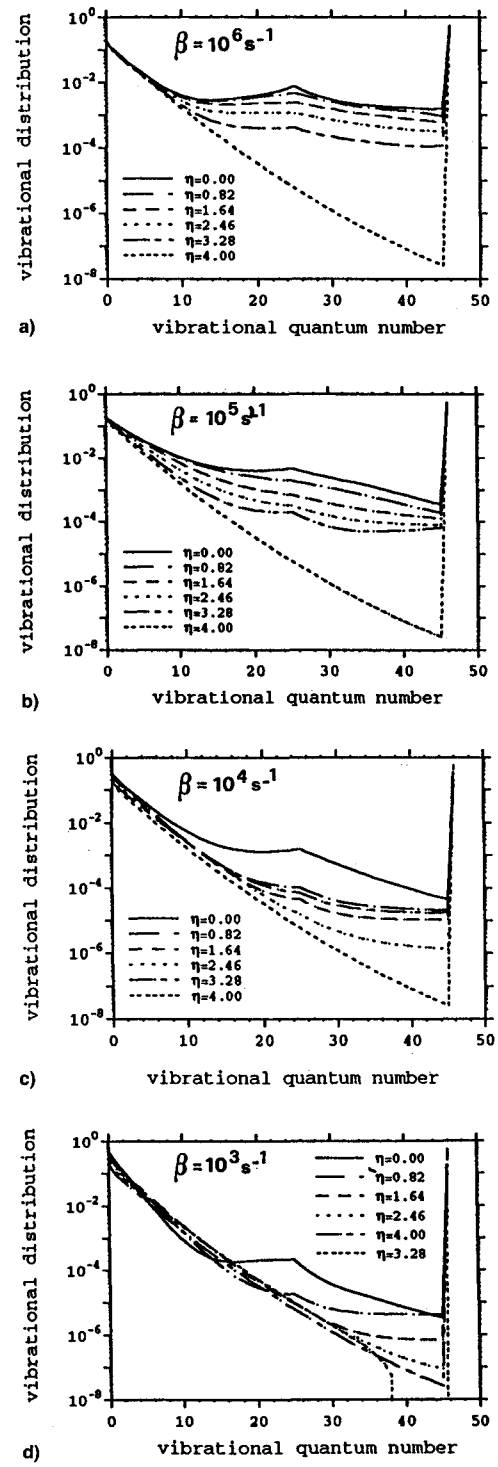

Fig. 6 Vibrational distributions vs vibrational quantum number at different η positions at fixed pressure ($p = 10^5$ N/m^2) and different β values calculated inserting V–V and V–T (by molecules) energy exchange processes and the recombination/dissociation kinetics ($T_t = 7000$ K and $T_v = 1000$ K).

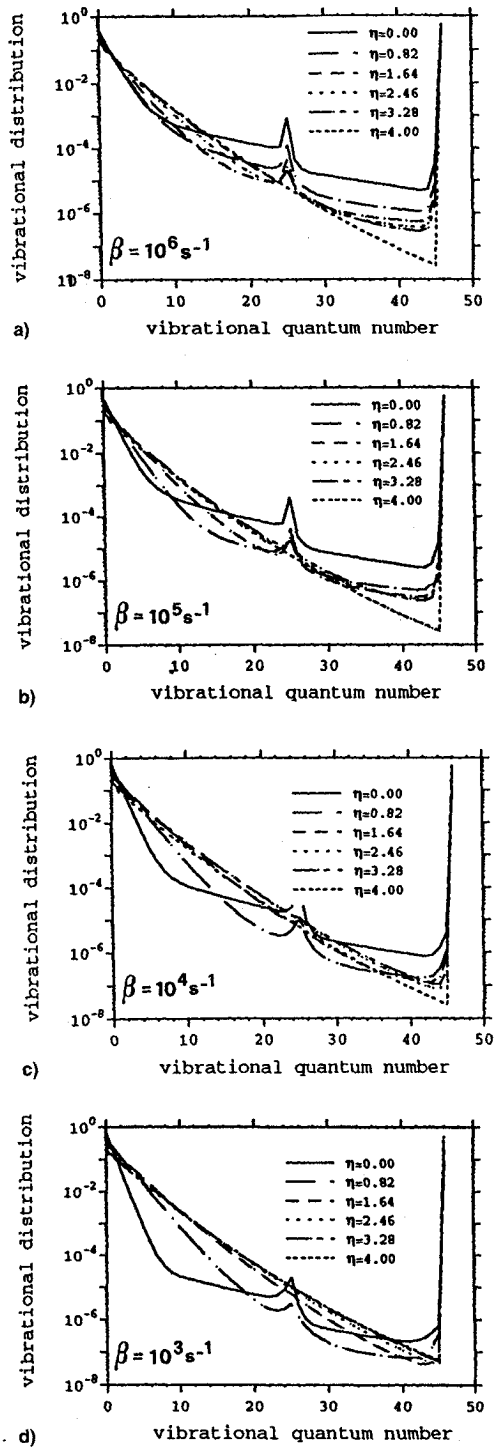

Fig. 7 Vibrational distributions vs vibrational quantum number at different η positions at fixed pressure ($p = 10^5$ N/m^2) and different β values calculated inserting V–V and V–T (by both atoms and molecules) energy exchange processes and recombination–dissociation kinetics ($T_e = 7000$ K and $T_w = 1000$ K).

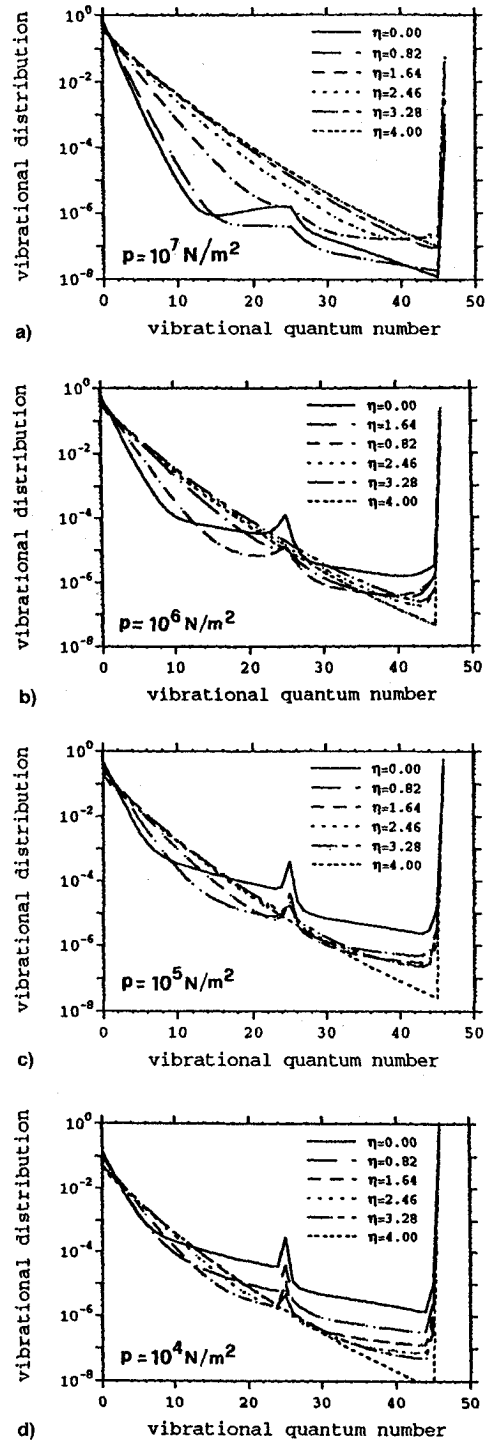

Fig. 8 Vibrational distributions vs vibrational quantum number at different η positions at fixed β ($\beta = 10^5$ s^{-1}) and different pressures calculated inserting V–V, V–T (by both atoms and molecules) energy exchange processes and recombination–dissociation kinetics ($T_e = 7000$ K and $T_w = 1000$ K).

frozen and the vibrational distribution is the same for all η values. Note also the strong overpopulation of vibrational levels near the surface, i.e., at low translational temperatures, when the V–V pumping mechanism[1] is such to create an inversion in vibrational distribution. For $\beta = 10^3$ s^{-1}, a Treanor distribution is formed. Under these conditions the temperature of the first vibrational levels remains frozen $T_1 = T_e$ so that near the surface $T_1 >> T(0)$.

Note that the narrow spike appearing for $v = 46$ represents the concentration of atomic nitrogen at different η values rather than the concentration of a given vibrational level. Under many conditions studied in the present work (see also Figs. 3–8) the concentration of atomic nitrogen can be considered frozen along η, so that a spike appears in this representation.

Figures 3a–3d report the effect of the pressure at a fixed β ($=10^5$ s^{-1}). At these conditions the Treanor distribution is reached only at very high pressure, when V–V relaxation times are shorter than β (remember that V–V kinetic terms are second-order with pressure).

Note also that results in Figs. 2a–2d and 3a–3d depend on the p/β ratio. As an example, the results of Fig. 2b are equal to the corresponding results reported in Fig. 3c.

Let us now consider the vibrational distributions in the presence of both V–V and V–T energy exchange processes. Figures 4a–4d report the vibrational distributions at fixed pressure and different β values. We can see that, only in proximity of the surface when T_1 is much higher than T, V–V processes push the vibrational distribution towards nonequilibrium. As an example, at $\beta = 10^4$ s^{-1}, for $v \geq 25$, the vibrational distribution adjacent to the surface ($\eta = 0$) is more populated than the corresponding ones at $\eta = 0.82$ and 1.64. Note that the last two distributions are locally equilibrated at a temperature higher than T_w (see Fig. 1a for the temperature profile).

Results at fixed β and different pressure values show that increasing the pressure makes the V–T processes dominate the V–V ones, therefore nonequilibrium effects in the vibrational distributions adjacent to the surface become less evident.

So far we have considered the vibrational kinetics including V–V and/or V–T processes, with the latter process concerning only collisions between molecules. At this point it is of great interest to examine the role of V–T energy exchanges involving molecule-atom collisions (i.e., process 15) on the vibrational kinetics. Still we disregard the recombination–dissociation processes. Figures 5a–5d report the corresponding vibrational distributions in the same conditions of Figs. (4a–4d), in which it is clearly shown that the introduction of V–T by atom collisions further increases the thermalization of the distributions.

Recombination–dissociation processes will radically change the vibrational kinetics, because of the selective pumping of the vibrational distribution. The first step is to introduce recombination–dissociation processes, neglecting at the same time the V–T processes by atoms. The results are reported in Figs. 6a–6d. We can see that the selective pumping at $v = 25$ and 45 (the last vibrational level) and the spread of this pumping over the whole vibrational manifold of N_2 through V–V and V–T processes creates vibrational distributions very far from equilibrium. The long plateau characterizing the distributions is because of the cooperation of recombination–dissociation and V–T processes, rather than a result of the redistribution of vibrational quanta by the V–V energy exchange. Note also that the long plateau tends to decrease with increasing the ratio p/β.

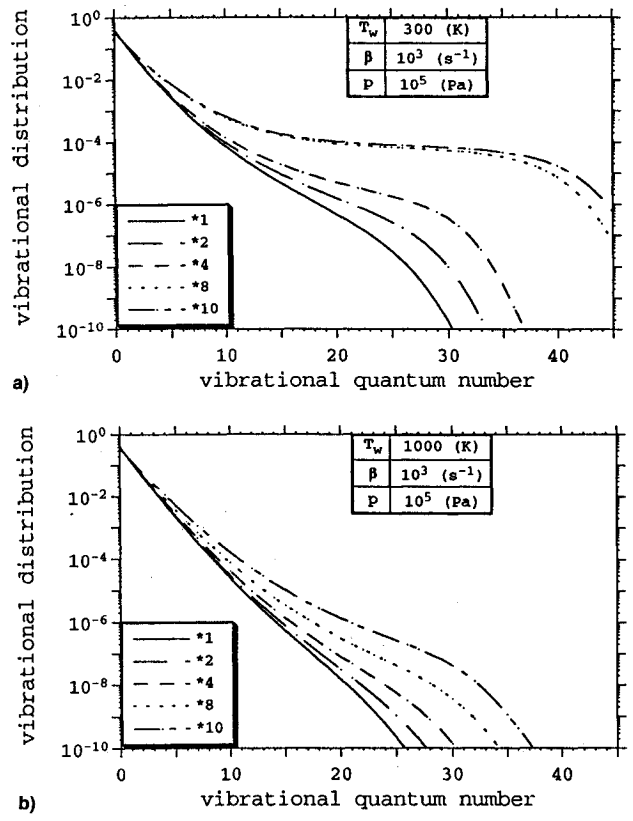

Fig. 9 Influence of V–V rate changes on the vibrational distributions near the surface ($\eta = 0$) for two wall temperature values. The different curves have been obtained by increasing by the reported values the V–V rates (the model includes only V–V and V–T rates).

Insertion of V–T by atoms in the whole kinetics cools down the vibrational distribution, as can be appreciated in Figs. 7a–7d and 8a–8d (see also Ref. 10). We note a strong increase of the peak at $v = 25$ as a consequence of the interplay of the different processes. Of course this peak is mainly because of the recombination model used in this work. Other models,[11] which do not consider the recombination of nitrogen atoms to electronically excited states, do not present this peak.

Before ending this section we want to remind the reader that the present results strongly depend on the sets of V–V and V–T rates used. As an example, Figs. 9a and 9b report the vibrational distributions of the N_2 adjacent to the surface ($\eta = 0$), obtained by changing the V–V rates (we include in this calculation only the V–V and V–T processes). A dramatic dependence of the vibrational distributions on the V–V rates is pointed out, particularly at $T_w = 300$ K. Note that, increasing the V–V rates produces a long plateau in the vibrational distributions, very similar to those reported by our group for discharge and postdischarge conditions.[1] A similar situation occurs, even if less dramatically, by changing the recombination–dissociation rates.

IV. Conclusions

In this article we have shown the nonequilibrium vibrational distributions of N_2 in the boundary layer surrounding a vehicle re-entering the atmosphere at a hypersonic speed. The nonequilibrium character of these distributions, when the complete kinetic model is considered, are mainly because of the selective pumping at the $v = 25$ and 45 levels from the recombination process, followed by the redistribution of vibrational quanta through V–V and V–T energy exchanges. Nonequilibrium effects strongly increase near the low-temperature surface.

The results strongly depend on the assumptions made in the model: in particular, considering a surface that is inert to either atom recombination or to the accommodation of vibrational energy, restricts the validity of this work to ceramic walls rather than to metallic ones. Moreover, the simplified fluid dynamics used in this work could limit the extension of these results to more realistic situations. In spite of these limitations we believe that the present model clarifies the role of nonequilibrium vibrational kinetics in re-entry problems. The uncertainties in both the chemical and fluid dynamic models used in the present work lead us to conclude that the present results are valid from a qualitative point of view.

Acknowledgments

This work has been partially supported by Agenzia Spaziale Italiana. We thank the referees for their helpful comments.

References

[1]Capitelli, M. (ed.), "Non-Equilibrium Vibrational Kinetics," *Topics in Current Physics*, Vol. 59, 1986, pp. 5, 96.

[2]Doroshenko, V. M., Koudriatsev, N. N., Novikov, S. S., and Smetanin, V. V., "Dependence of Heat Transfer on the Formation of Vibrationally Excited Nitrogen Molecules During the Recombination of Atoms in a Boundary Layer," *High Temperature*, Vol. 28, No. 1, 1986, pp. 70–75.

[3]Armenise, I., Capitelli, M., Colonna, G., Koudriatsev, N. N., and

Smetanin, V. V., "Non-Equilibrium Vibrational Kinetics During Hypersonic Flow of a Solid Body in Nitrogen and Its Influence on the Surface Heat Transfer," *Plasma Chemistry Plasma Processing*, Vol. 15, No. 3, 1995, pp. 501–528.

[4]Anderson, J. D., "Hypersonic and High Temperature Gas Dynamics," McGraw–Hill, New York, 1989.

[5]Aganov, V. P., Vertuchlyn, V. K., Gladkov, A. A., and Polianskii, O. Yu., "Nonequilibrium Physical and Chemical Processes in Aerodynamics," *Machinostroenie*, Moscow, 1972 (in Russian).

[6]Capitelli, M., Gorse, C., and Billing, G. D., "V-V Pumping up in Non-Equilibrium Nitrogen: Effects on the Dissociation Rate," *Chemical Physics*, Vol. 52, No. 3, 1980, pp. 299–304; also Billing, G. D., and Fisher, E. R., "VV and VT Rate Coefficients in N2 by a Quantum-Classical Model," *Chemical Physics*, Vol. 43, No. 4, 1979, pp. 395–401.

[7]Laganà, A., and Garcia, E., "Temperature Dependence of N+N2 Rate Coefficients," *Journal of Physical Chemistry*, Vol. 98, No. 2, 1994, pp. 502–507.

[8]Armenise, I., Capitelli, M., Celiberto, R., Colonna, G., Gorse, C., and Laganà, A., "The Effect of N+N2 Collisions on the Non-Equilibrium Vibrational Distributions of Nitrogen Under Reentry Conditions," *Chemical Physics Letters*, Vol. 227, Nos. 1,2, 1994, pp. 157–163.

[9]Park, C., "Non-Equilibrium Hypersonic Aerothermodynamics," Wiley, New York, 1990.

[10]Armenise, I., Capitelli, M., Celiberto, R., Colonna, G., and Gorse, C., "Non-Equilibrium Vibrational Distributions of N2 Under Reentry Conditions: The Role of Atomic Nitrogen," AIAA Paper 94-1987, June 1994.

[11]Armenise, I., Capitelli, M., and Gorse, C., "On the Coupling of Non-Equilibrium Vibrational Kinetics and Dissociation-Recombination Processes in the Boundary Layer Surrounding Hypersonic Reentry Vehicle," European Space Agency SP-367, Nordvijk, The Netherlands, 1995, pp. 287–292.